Estimation of Large Frequency Offsets using 5 GHz WLAN Training Symbols

Kai-Uwe Schmidt[+], Markus Mück[++], Xavier Miet[++], and Jens Schönthier[+]

[+]Dresden University of Technology, Communications Laboratory
01062 Dresden, Germany – Email: {schmidtk, schoenthier}@ifn.et.tu-dresden.de

[++]Motorola Labs France, Espace Technologique Saint Aubin
91193 Gif-Sur-Yvette, France – Email: {markus.muck, xavier.miet}@crm.mot.com

ABSTRACT

This paper discusses the estimation and correction of large frequency offsets in the context of OFDM based WLANs such as BRAN HIPERLAN/2 and IEEE802.11a. Several algorithms with different complexity/performance trade-offs are proposed, all based on the exploitation of frequency domain properties of standard burst preambles: A correlation based approach leads to optimum performances at a moderately high cost while simple unit- or zero-carrier detection will lead to sub-optimum, but very low-cost implementation schemes. In the framework of the IST BROADWAY project[1], this technique is used in order to keep compatibility to 5 GHz WLAN standards at a carrier frequency of 60 GHz where large frequency offsets occur. Simulation results prove that a 20 ppm offset at 60 GHz is detected at a high reliability.

Keywords: frequency offset estimation, BRAN HIPERLAN/2, IEEE802.11a, IST BROADWAY, 60 GHz

I. INTRODUCTION

Orthogonal Frequency Division Multiplexing (OFDM) is the chosen modulation scheme of modern high-data rate communication systems (xDSL, DAB, DVB-T, BRAN HIPERLAN/2, IEEE802.11a/g, IEEE802.15.3a, considered for 4G, etc.). In the context of WLANs, current data rates (54 Mbps on top of the physical layer) are foreseen to be insufficient for very dense urban deployment, such as for hot spot coverage. This is the motivation for IEEE to propose and specify in the scope of the IEEE802.11n (former High Throughput Study Group) solutions for very high data rates WLANs (targeting at least 100Mbps on top of the MAC layer) in the 5 GHz band. Another path is to investigate higher frequency bands where more spectrum is available such as the 60 GHz approach in the framework of the IST-2001-32686 BROADWAY Project [1], [2].

BROADWAY proposes a hybrid dual frequency system operating at 5 GHz based on ETSI BRAN HIPERLAN/2 [3] and at 60 GHz through an innovative full ad-hoc extension named HIPERSPOT. This enables the use of larger bandwidths resulting in higher data rates. In order to ensure a smooth transition from 5 GHz WLANs to the 60 GHz band, 5 GHz PHY layer compatible modes are introduced at 60 GHz as well as new modes guaranteeing high throughput and mobility. On the other hand, the design of the RF frontend is a main challenge. In particular, the frequency deviation of the local oscillators will rise up linearly with the carrier frequency if the relative accuracy of the oscillators remains unchanged. In order to ensure low-cost RF devices even at high frequencies, extended base-band algorithms are required to estimate and compensate large frequency offsets. This is particularly true for the modes compatible to 5 GHz PHY layers, since the corresponding preambles were not designed for 60 GHz needs. This paper proposes algorithms ensuring an efficient estimation and correction of large frequency offsets using the classical BRAN HIPERLAN/2 [3] or IEEE802.11a [4] preamble structure.

Considering existing techniques, [5] and [6] discuss standard frequency offset estimation based on the detection of a linear phase in time domain due to the frequency offset. These approaches are commonly used in the 5 GHz band. In the presence of very large offsets, this technique is insufficient, since a phase ambiguity of integer multiples of $\pm\pi$ arises. [7] and [8] propose an efficient algorithm that imposes a differentially modulated PN-sequence as preamble. After a first offset correction based on standard techniques, the remaining ambiguities are resolved by identifying a shift in frequency domain in the differentially decoded preambles. Another proposal of the same authors [9] is feasible for a larger variety of preambles, but imposes constraints on the OFDM symbol size N and the guard interval size D. They must be mutually prime in order to ensure the optimum detection range. These constraints are unfortunately incompatible with standard WLAN systems. [10] proposes to identify the remaining ambiguities after a first estimation/correction step by correlation or zero carrier detection. However, the study is limited to very particular designs of preambles. In our paper, the frequency offset estimation and detection mechanisms are extended to the needs of standard WLAN preambles.

This paper is organized as follows. In section II we briefly discuss the effects of small and large carrier frequency offsets on the received OFDM signal. Also a short overview of the considered preamble structure is given. The common frequency offset estimation approach using the considered WLAN preambles is shortly introduced in section III. In section IV we propose some algorithms that enable the estimation of arbitrary large frequency offsets. In section V some simulation results are presented. Section VI concludes the paper.

[1] This work is supported by the European Commission in the scope of the IST BROADWAY project IST-2001-32686 [1].

II. PRELIMINARY

In an OFDM system N orthogonal sub-carriers are employed. Each of the sub-carriers operates at the sub-carrier frequency $f_k = f_c + (k - N/2) f_s$, $(k = 0,\ldots,N-1)$, with f_s being the sub-carrier spacing and f_c the carrier frequency, and it is modulated with the complex amplitude X_k. In order to maintain orthogonality, the time-domain signal is usually obtained by an inverse discrete FOURIER transform (IDFT)

$$x_n = \frac{1}{\sqrt{N}} \sum_{k=0}^{N-1} X_k e^{j2\pi f_k T_s}, \quad n = 0,1,\ldots,N-1, \tag{1}$$

where $T_s = 1/Nf_s$ is the sampling period. To prevent inter-symbol interference, the time-domain signal of the OFDM symbol is preceded by a guard interval. This can be either (i) a blank field (zero padding) [11], (ii) a cyclic prefix [11], or (iii) a fixed signal [12] and should be longer than the maximum delay of the channel. In the following we will focus on the standard cyclic prefix case. After passing the signal through a multipath channel and removing the guard interval, at the receiver the complex signal amplitude of the k^{th} sub-carrier is found by a discrete FOURIER transform (DFT)

$$Y_k = \frac{1}{N} \sum_{n=0}^{N-1} \sum_{l=0}^{N-1} H_l X_l e^{j2\pi n (f_l - f_k') T_s} + V_k, \tag{2}$$

where H_k are the frequency domain channel coefficients and V_k is the GAUSSian noise transformed into frequency domain. Note that in the receiver the sub-carrier frequencies are f_k' rather than f_k. This is because they were not generated by the same oscillator and so are in general distinct. We say, the receiver sub-carrier frequencies deviate by an offset of Δf from the transmitter sub-carrier frequencies. Then we can write:

$$\Delta f = f_k' - f_k = \Delta k\, f_s \quad \text{with} \quad \Delta k = \Delta + \delta, \tag{3}$$

where Δ is integer and $|\delta| \le \frac{1}{2}$. That means Δ denotes the frequency deviation of a multiple of the sub-carrier spacing and δ is the frequency deviation of a fraction of half the sub-carrier spacing.

With all these preliminaries and some modification steps one can rewrite (2)

$$Y_k = \frac{1}{N} \sum_{l=0}^{N-1} H_{l-\Delta} X_{l-\Delta} \frac{\sin(\pi\delta)}{\sin\left(\pi \frac{l-k+\delta}{N}\right)} \frac{e^{j\pi\delta(N-1)/N}}{e^{j\pi(l-k)/N}} + V_k \tag{4}$$

with the convention $H_k X_k = H_{k+iN} X_{k+iN}$ for i integer. This equation motivates to draw some important conclusions. The received OFDM symbol in frequency domain is shifted cyclically by Δ sub-carrier spacings. That means the case $\Delta \ne 0$ leads to a complete loss of the data. Now consider the case $\Delta = 0$, $\delta \ne 0$, and $l = k$. Then the received amplitude of the sub-carrier k is attenuated by a complex factor. In case $\Delta = 0$, $\delta \ne 0$, and $l \ne k$ the sub-carrier k is distorted by interference coming from all other sub-carriers. Thus it is mandatory to detect the integer part of the frequency offset correctly and estimate the fractional part of the frequency offset with sufficient accuracy.

We close this section with a brief presentation of the relevant parts of the considered preambles that will be used in the algorithms presented in this paper. A detailed description of the preambles is given in [3], [4]. In Fig. 1 the sub-carrier assignment for the B- and the C-field is shown systematically.

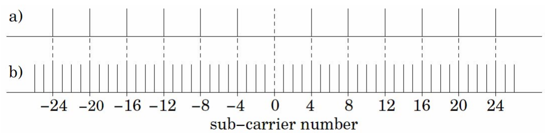

Fig. 1: Sub-carrier assignment for the a) B-field and b) C-field

Note that in the B-field only every fourth sub-carrier is used, leading to a periodic time-domain signal with period $N/4$. The B-field sub-carriers are modulated with $\pm\sqrt{2}(1+j)$ and C-field sub-carriers are modulated with ± 1. The DC sub-carrier and some side sub-carriers are not used at all. In the remainder of this paper we will refer to the B-field and the C-field sub-carriers with $\mathbf{X}^B$ and $\mathbf{X}^C$, respectively. X_k denotes the k^{th} element of $\mathbf{X}$.

III. CLASSICAL FREQUENCY OFFSET ESTIMATION IN 5 GHZ WLANS

From (1) one can see that the transmitted signal is generated with the sub-carrier frequencies f_k and in (2) the received signal is interpreted at the sub-carrier frequencies f_k'. That means the spectrum of the received signal is shifted by the frequency difference Δf. Then we receive

$$r_n = y_n e^{j2\pi n \Delta f T_s}, \tag{5}$$

where y_n would be the received signal without a frequency deviation, i.e. it is the cyclic convolution of the transmitted signal with the channel impulse response plus some noise.

Now we briefly describe how an estimate of the frequency offset Δf can be obtained by estimating the linear phase shift in time domain. In order to be able to employ this scheme, a training sequence comprising several, say $(M-1)$, repetitions of a sub-sequence of length d is required. Then the auto-correlation value at a displacement d is calculated

$$\Gamma = \sum_{n=0}^{W-1} r_n^* r_{n+d}, \tag{6}$$

where W is the window size and $(.)^*$ is the complex conjugate. Clearly with $W = Md$ one can estimate the frequency offset by

$$\hat{\Delta} f = \arg(\Gamma) / 2\pi d T_s, \tag{7}$$

where $\arg(.)$ determines the phase of a complex number. Obviously the accuracy of the estimate becomes better as W increases. The $\arg$-function yields only a unique value if the real phase of the argument is within the interval $[-\pi, +\pi)$. Then from (7) follows that if

$$-1/2dT_s \le \Delta f < 1/2dT_s, \tag{8}$$

then the estimation of the frequency offset is unique.

Let us consider now the case where the 5 GHz WLAN training symbols are used for the frequency offset estimation. We have several choices for the estimation parameters, depending on which part of the preamble is used. Some Options and the resulting acquisition range according to (8) are summarized in Table I.

Table I: Possible parameter Options for the 5 GHz WLAN preambles

Option	Field	d	W	M	range
I	B-field	16	16	1	$-2f_s \ldots +2f_s$
II	B-field	16	48	3	$-2f_s \ldots +2f_s$
III	B-field	32	32	1	$-f_s \ldots +f_s$
IV	C-field	64	64	1	$-f_s/2 \ldots +f_s/2$

The largest frequency offset that can be uniquely estimated is $\pm 2 f_s$. According to [3] and [4] the maximum allowed relative frequency deviation of both the transmitter and the receiver oscillator is 20 ppm. With a maximum carrier frequency of 5.7 GHz the maximum possible frequency offset that can occur is 228 kHz. Obviously this lies within the acquisition range of the scheme described above, but if we aim at higher carrier frequencies without sacrificing the convenience of low-cost RF devices, extended algorithms are required.

IV. ESTIMATION OF ARBITRARY LARGE FREQUENCY OFFSETS

A. Principle:

For the considerations in this subsection we assume a noiseless transmission. Following the argumentation leading to (8) one can show that the estimation of a frequency offset Δf with the phase difference estimator would yield

$$\hat{\Delta f} = \left(\Delta f + 1/2dT_s\right) \bmod \left(1/dT_s\right) - 1/2dT_s \qquad (9)$$

where mod is the modulus operation. Now we assume $\delta = \delta \bmod N/2d$, which holds for $d \le N$. Then after the frequency offset estimation with (7) and its compensation a frequency offset of

$$\Delta f - \hat{\Delta f} = f_s \left[\Delta + \frac{N}{2d} - \left(\Delta + \frac{N}{2d} \right) \bmod \frac{N}{d} \right] = f_s \Delta' \quad (10)$$

remains. Clearly under the premise $d \le N$ the fractional part δ has been estimated correctly. The problem is now reduced to detect the integer part Δ' when $\delta = 0$. Then we can write (4) as

$$Y_k = H_{k-\Delta'} X_{k-\Delta'}, \qquad (11)$$

where the convention associated with (4) still holds.

From Table I one can see that for the considered training symbols d can be 16, 32, or 64. Using (10) the possible remaining frequency offsets can be calculated. We define the set $\mathbf{L}$ comprising all possible values for Δ' with the constraint that the largest absolute value is determined by the maximum frequency offset that can occur. For example $d = 64$ implies that Δ' can be an arbitrary integer and for $d = 16$ possible values are $\{\ldots, -8, -4, 0, 4, 8, \ldots\}$. Thus when decreasing d some values can be excluded. In order to keep the complexity of the detection algorithm low, we propose to perform the initial frequency offset estimation with the B-field and set $d = 16$. The estimation might be further refined by exploiting the C-field.

In the next two subsections we will present two algorithms to detect the remaining cyclic frequency shift Δ'.

B. The Correlation Approach:

Let $\mathbf{Y}^B$ and $\mathbf{Y}^C$ be the reconstructed vectors of $\mathbf{X}^B$ and $\mathbf{X}^C$ at the receiver (i.e. by applying the DFT on the appropriate received preamble sequences).

Then one may calculate a metric

$$\Lambda(l) = \sum_{k=0}^{N-1} \frac{X_k^B}{X_k^C} Y_{k+l}^C Y_{k+l}^{B\,*} \qquad (12)$$

for all $l \in \mathbf{L}$. By taking (11) into account one can see clearly that Λ has a maximum for $l = \Delta'$, so

$$\hat{\Delta}' = \arg\max\left(\Lambda(l)\right). \qquad (13)$$

Obviously the performance of this scheme depends on the correlation properties of $\mathbf{X}^B$ and $\mathbf{X}^C$. Since $\mathbf{X}^C$ comprises only ± 1, it holds $X_k^C = 1/X_k^{C\,*}$. Then we can consider X_k^B / X_k^C as elements of a differentially modulated symbol and hence the performance directly depends on the autocorrelation properties of this symbol. In that form this algorithm is formally identical to the algorithm proposed by SCHMIDL and COX [7], but it has some benefits in terms of implementation complexity. By making some variable substitutions and using the fact that $X_k^B = \{0, \pm\sqrt{2}\,(1+j)\}$ and $X_k^C = \{0, \pm 1\}$ we can write (12) as

$$\begin{aligned}\Lambda(l) = & \sum_{k|X_{k-l}^B \neq 0} \operatorname{sign}\left[\Re\left\{ \frac{X_{k-l}^B}{X_{k-l}^C} \right\} \right] \\ & \left[\left(\Re\left\{ Y_k^C Y_k^{B\,*} \right\} - \Im\left\{ Y_k^C Y_k^{B\,*} \right\} \right) \right. \\ & \left. + \; j \left(\Re\left\{ Y_k^C Y_k^{B\,*} \right\} + \Im\left\{ Y_k^C Y_k^{B\,*} \right\} \right) \right],\end{aligned} \qquad (14)$$

where $\Re\{.\}$ is the real and $\Im\{.\}$ the imaginary part of a complex number. That means the first term can be precomputed for each $l \in \mathbf{L}$ and stored in a look-up table and the other terms need to be computed only once, since they do not depend on l. Then for each $l \in \mathbf{L}$ only sign manipulations and additions have to be carried out.

C. The Power Detection Approach:

In the following we focus on $\mathbf{Y}^B$, the reconstructed vector of $\mathbf{X}^B$. From (11) one can see that the elements of this vector are complex attenuated and shifted cyclically. Now $\mathbf{Y}^B$ may be compared with $\mathbf{X}^B$. In Fig. 1 one can see that $\mathbf{X}^B$ is non-zero at every fourth sub-carrier except at the DC sub-carrier and some side sub-carriers. At the receiver $\mathbf{Y}^B$ is shifted cyclically by l samples and the total power on the sub-carriers that are supposed to be non-zero is calculated by

$$\Omega(l) = \sum_{k|X_k^B \neq 0} \left| Y_{k+l}^B \right|^2 \qquad (15)$$

for each $l \in \mathbf{L}$. The metric Ω should reach its maximum when $l = \Delta'$. Hence

$$\hat{\Delta}' = \arg\max\left(\Omega(l)\right). \qquad (16)$$

By expanding (15) and (12) one can see that for a pure AWGN channel with high SNR this approach roughly coincides with the algorithm presented in the latter subsection.

The summation in (15) implies 11 additions (since $\mathbf{X}^B$ comprises 12 non-zero elements). If we assume that the initial estimation of the frequency offset was performed with the B-field and $d=16$ was used, the number of additions might be reduced. Then, following (10), $\mathbf{L}$ comprises only values of multiples of 4. That means the received symbol $\mathbf{Y}^B$ has to be shifted only by multiples of 4. Hence, only 16 out of 64 samples of $\mathbf{Y}^B$ will be considered, where in the absence of noise 4 samples are zero and 12 samples are non-zero. Now one can detect the shift by computing the total power at the sub-carriers that are supposed to be zero

$$\Theta(l) = \sum_{k|X_k^B \neq 0} \left|Y_{k+l}^B\right|^2 , \quad (17)$$

where the minimum of Θ should occur when $l=\Delta'$. Hence

$$\hat{\Delta}' = \arg\min\left(\Theta(l)\right). \quad (16)$$

Under the assumption $d=16$ was used for the initial estimation it is clear that (18) will yield exactly the same result as (16). This way the number of additions is reduced from 11 to only 3 for each $l \in \mathbf{L}$.

V. SIMULATION RESULTS AND DISCUSSION

In order to demonstrate the performance of our proposed schemes, simulations have been carried out. Since we aim to reuse the 5 GHz WLAN training symbols at high carrier frequencies, we will show some results for the 5 GHz as well as for the 60 GHz case. At 5 GHz the ETSI-BRAN A [13] channel model is used and at 60 GHz we employ a channel model considered in [14], where it is referred to as TUD-NLOS1. This model has taps at {0,15,20,35,40,45, 55,70} ns with a relative attenuation {0,–10,5,–10,–10,0, –15,–8} dB, respectively. Note that in general the 60 GHz channels become considerable short. Both channel models are designed for a similar office environment with non-line of sight (NLOS) between the transmitter and receiver antenna, so the amplitude of each tap is RAYLEIGH distributed. In our simulations we normalize the channel impulse response so that the total received power is equal to one.

In order to asses the performance of our schemes one has to take into account (i) the accuracy of the frequency offset estimation if the detection of Δ' was correct and (ii) the detection failure probability of Δ'. The accuracy of the estimation is then completely given by the performance of the phase difference estimator and often indicated by the mean square error $\mathrm{MSE}[\widehat{\Delta f}] = \| \widehat{\Delta f} - \Delta f \|^2$. In the appendix of this paper we show that the MSE is rather independent on the channel, because the performance only depends on the total received power. In Fig. 2 the normalized MSE is plotted over the SNR for three Options from Table I. The lines indicate theoretical results, derived in [6] and in the appendix of this paper. Stars indicate the according simulated values. For the solid line we assumed $\Delta k = 0 \bmod N/2d$ and the dashed line stands for $\Delta k = 1.7 \bmod N/2d$ for Option I and II and $\Delta k = 0.3 \bmod N/2d$ for Option IV. The difference between the solid and the dashed lines is because this estimator is biased [6]. There is a good correspondence between theoretical and simulation results for Option I and IV. As presented in the appendix of this paper the theoretical results for $M>1$ are based on an approximation for high SNR. For Option II the gap between theory and simulation becomes quite small for reasonable SNR.

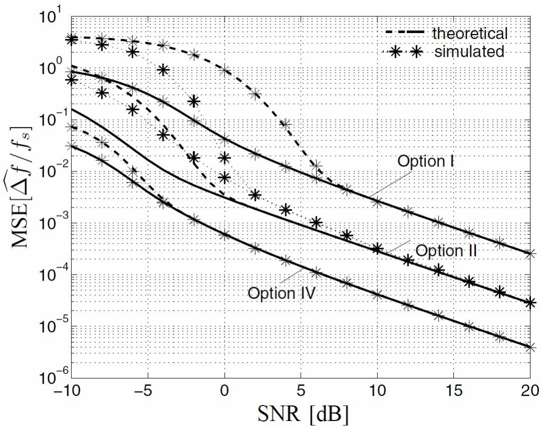

Fig. 2: Mean square error of the initial frequency offset estimation

For the detection failure simulations we assume an oscillator accuracy of 20 ppm at 60 GHz. Hence the maximum frequency offset that can occur is 7.68 sub-carrier spacings. Note that this is equivalent to a tolerable oscillator accuracy of 480 ppm at 5 GHz. In our simulations the frequency offset is uniquely distributed within the interval $[-7.68, +7.68] f_s$ and we perform the initial frequency offset estimation with Option II from Table I. Following (10) after the initial estimation it remains a frequency offset of either {–8,–4,0,4,8} sub-carrier spacings. It is now the aim of the detection algorithm to find the correct frequency shift. The performance of the proposed algorithms is measured in terms of their detection failure probabilities. In Fig. 3 the results are shown for the AWGN, the ETSI-BRAN A and the TUD-NLOS1 channel model.

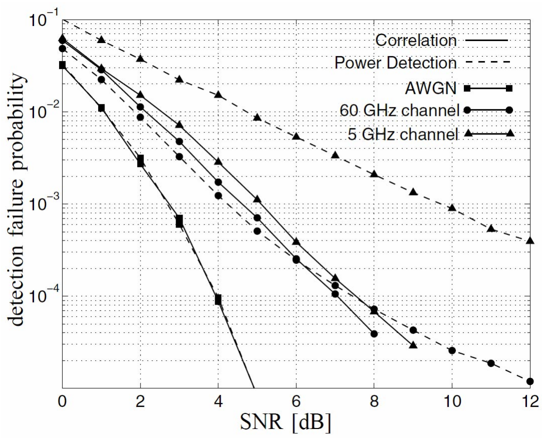

Fig. 3: Detection failure probability of the frequency offset detection

As predicted in section IV for the AWGN channel model both algorithms behave very similar. In fact both curves are on top of each other. More general, we observe that for short channels the performance of both algorithms is close to each other. When the channel delays become longer, the curves for the power detection algorithm flatten with an increasing SNR. For the TUD-NLOS1 channel model this happens at quite high SNR, but for the ETSI-BRAN A channel model the performance penalty is about 5 dB at 10^{-3}. Note that even this is still acceptable for many applications, in particular when low complexity counts.

Let n be the number of elements in $\mathbf{L}$ and assume the initial estimation was performed with $d = 16$. Then the power detection algorithm requires only $3n$ complex additions, while the correlation algorithm requires 12 complex multiplications and $3 + 12n$ complex additions. Both algorithms need one additional FFT to obtain $\mathbf{Y}^B$ ($\mathbf{Y}^C$ is usually available). Thus the accuracy of the correlation algorithm goes on the cost of considerable more complexity.

VI. CONCLUSIONS

Based on the 5 GHz WLAN training symbols we presented a way to estimate frequency offsets beyond the restrictions of the according system standards. The problem is reduced to a detection of a frequency shift that is a multiple of the sub-carrier spacing. It was shown that the considered preambles are suitable to apply the SCHMIDL and COX algorithm. Due to the simple structure of the preambles the algorithm is modified leading to much lower complexity. Furthermore we proposed a very simple scheme that relies on sub-carrier power detection. The latter one is very suitable as a low-cost solution and is in particular powerful for short channels. The proposed schemes also offer the ability to use low-cost oscillators for systems in the 5 GHz range, as it would be the case in low-cost Personal Area Network (PAN) systems that are compatible with existing WLAN standards.

APPENDIX

Comments on the Statistical Performance of the Phase Difference Estimator:

We briefly present some results for the distribution of the estimated phase in the presence of GAUSSian noise. These results extend the results of [6], [15] for $M > 1$. The probability distribution function (PDF) of the estimated phase $\hat{\phi} = \arg(\Gamma)$ (see (7)) under condition ϕ is

$$f_\Gamma\left(\hat{\phi} \mid \phi\right) = \frac{\sqrt{2M-1}}{2\pi\gamma} e^{-\rho \frac{M}{2M-1}} + \frac{1}{2}\sqrt{\frac{M}{\gamma^3 \pi}} \sqrt{\rho} \cos\left(\hat{\phi} - \phi\right) e^{-\rho \frac{M \sin^2\left(\hat{\phi}-\phi\right)}{\gamma}} \left[1 + \operatorname{erf}\left(\sqrt{\rho} \cos\left(\hat{\phi} - \phi\right) \sqrt{\frac{M}{\gamma(2M-1)}}\right)\right], \tag{19}$$

with

$$\gamma = M - (M-1)\cos\left(2\left(\hat{\phi} - \phi\right)\right),$$

$$\operatorname{erf}(x) = \frac{2}{\sqrt{\pi}} \int_0^x e^{-z^2} dz, \quad \text{and} \quad \rho \approx \frac{W P_s}{2\sigma^2},$$

where P_s is the signal power and σ^2 the variance of the complex GAUSSian noise. In case $M = 1$ one can use

$$\rho = \left(W P_s^2 / \sigma^4\right) / \left(2 P_s / \sigma^2 + 1\right) \quad | \quad M = 1$$

and hence get the exact distribution in (19). The reason for the approximation is that for $M > 1$ it is tough to find the exact solution for f_Γ. So we have to rely on this approximation which delivers quite accurate solutions for $P_s / 2\sigma^2 \geq 5\,\mathrm{dB}$. For $M = 1$ the distribution in (19) coincides with that in [6], [15] (where it is usually given as a FOURIER series). From (19) various characteristics, such as mean error, variance, and mean square error (MSE) of $\hat{\phi}$ and Δf may be derived.

ACKNOWLEDGEMENT

Note that the BROADWAY project is funded by the IST Information Society Technologies program of the European Commission (see `http://europa.eu.int/information_society`).

The authors would like to acknowledge all the partners of the project for their valuable contributions and discussions: These are Motorola Labs France, Dresden University of Technology, IMST and IRK Germany, TNO FEL Netherlands, INTRACOM and University of Athens Greece and FARRAN Ireland.

REFERENCES

[1] M. de Courville, S. Zeisberg, M. Muck, and J. Schönthier, "Broadway, the way to broadband access at 60 GHz", *IST Mobile Summit*, 2002.

[2] IST BROADWAY *official public Internet Web-Site*, `http://www.ist-broadway.org`.

[3] *ETSI TS 101 475: BRAN, HIPERLAN Type 2, Physical (PHY) Layer, Technical Specification*.

[4] IEEE 802.11, "Wireless LAN Medium Access Control (MAC) and Physical Layer (PHY) specifications", standard, IEEE Standards Department, New York, November 1997.

[5] P. H. Moose, "A technique for orthogonal frequency division multiplexing frequency offset correction", *IEEE Trans. Commun.*, vol. 42, pp. 2908-2914, October 1994.

[6] P. Sapiano and J. Martin, "Statistical performance of the first order phase difference digital instantaneous frequency estimator", *Electron. Lett.*, vol. 32, pp. 1657-1658, August 1996.

[7] T. M. Schmidl and D. C. Cox, "Robust frequency and timing synchronization for OFDM", *IEEE Trans. Commun.*, vol. 45, pp. 1613-1621, December 1997.

[8] T. M. Schmidl and D. C. Cox, "Low-overhead, low-complexity [burst] synchronization for OFDM", in *Conference Record of the International Conference on Communications (ICC)*, June 1996.

[9] T. M. Schmidl and D. C. Cox, "Blind synchronization for OFDM", *Electron. Lett.*, vol. 33, January 1997.

[10] Z. Dlugaszewski and K. Weselowski, "Simple coarse frequency offset estimation scheme for OFDM burst transmission", in *Proc. of the Int. Symposium on Personal, Indoor and Mobile Radio Communications PIMRC*, 2002.

[11] B. Muquet, Z. Wang, G. B. Giannakis, M. de Courville, and P. Duhamel, "Cyclic prefixing or zero padding for wireless multicarrier communications?", *IEEE Trans. Commun.*, December 2002.

[12] M. Muck, M. de Courville, M. Debbah, and P. Duhamel, "A pseudo random postfix OFDM modulator and inherent channel estimation techniques", in *GLOBECOM conference records*, San Francisco, USA, December 2003.

[13] *ETSI EP BRAN 3ERI085B: Channel Models for HIPERLAN/2 in Different Indoor Scenarios*, March 1998.

[14] J. Schönthier, "*The 60 GHz Channel and its Modelling*", IST-2001-32686, `http://www.ist-broadway.org`.

[15] B. Lovell and R. Williamson, "The statistical performance of some instantaneous frequency estimators", *IEEE Trans. Signal Proces.*, vol. 40, pp. 1708-1722, July 1992.